Geophys. J. Int. (1998) **135,** 438–448

Variations of stress directions in the western Alpine arc

E. Eva and S. Solarino*

Dipartimento di Scienze della Terra, University of Genova, Viale Benedetto V, 5 *Genova, Italy. E-mail: elena@dister.unige.it*

Accepted 1998 June 5. Received 1998 May 6; in original form 1997 September 5

SUMMARY

The western Alpine arc originated during the Cretaceous orogenesis as a consequence of the continental collision between the European and Adriatic plates. The distribution of forces acting in this sector of the Alps is still somewhat uncertain. In the past, some efforts have been made to map the distribution of P and T axes but it is known that these can be substantially different from the principal stress directions.

In recent work, we presented a first attempt to determine the directions of σ_1 and σ_3, which we could compute only for a 'local' regime at the level of the magnitude of the larger events that occurred in the area. To obtain the stress orientation, we applied the technique developed by Gephart and Forsyth to invert fault plane solutions.

In this work we present the results of a detailed analysis performed on a larger area, applying the same methodology. A total of 86 earthquakes with magnitudes ranging from 2.5 to 5.3 has been used for inversion. The results confirm the impossibility of defining, within the available data, a regional stress field. In fact, different local behaviours have been demonstrated in four subregions. For the first subregion, namely the northern part of the western Alps, the inversion of 28 earthquakes, resulting in a misfit of 5.9°, revealed a distensive regime orientated N–S. For the second subregion, the outer part of the western Alps, the inversion of 16 earthquakes led to a misfit of 5.3° for a distensive E–W orientated regime. In the inner part of the chain, an opposite result was obtained by the inversion of 14 earthquakes, confirmed by a misfit of 4.7°. Finally, the region of the Ligurian Sea revealed an almost horizontal NW–SE orientated σ_1, whereas σ_3 is NE–SW orientated with a dip of around 30°–40°. The inversion for this subarea was carried out on a data set of 28 earthquakes and characterized by a misfit of 7.1°. The uncertainty of the stress axis orientation (90 per cent confidence limits) is, on average for all inversions, around 40°.

Key words: fault plane solutions (FPS), seismotectonics, stress distribution.

INTRODUCTION

Since the early 1980s, the western Alpine arc has undergone a thorough seismic monitoring. The aim was to improve the understanding of this sector of the Alps, which originated during the Cretaceous orogenesis as a consequence of the continental collision between the European and Adriatic plates.

The development in the last decade of a large number of recording instruments and the increased accuracy of earthquake locations have evidenced the main trend of seismicity for this area (Fig. 1) (Eva *et al.* 1990).

In the Swiss sector of the studied area, seismicity is mainly located in the Valais region, where very strong earthquakes have occurred in the past (Mayer-Rosa & Mueller 1979). In the western Alps, seismic activity, consistent and of low magnitude, is mainly concentrated around the border between France and Italy. In this area, seismicity seems to be organized into two branches that clearly reflect the tectonic sketch, being almost coincident, within the location errors, with the Penninic front and the border of the Penninic unit and the Po plain. The external crystalline massifs appear as aseismic units and the seismic activity is concentrated along their margin. In the Ligurian Sea, seismicity is mainly located at the western side at the foot of the continental margin, although a seismic-swarm-like activity affects the inland region.

The recognition of these seismic behaviours is very important for the definition of subareas of homogeneous characteristics, as emphasized in the following.

Although the tectonic aspects of the formation and evolution of the orogen and the associated seismicity are now fairly well known, the distribution of forces currently acting and, as a

* Now at: Institut für Geophysik, ETH Hönggerberg, CH-8093 Zürich, Switzerland.

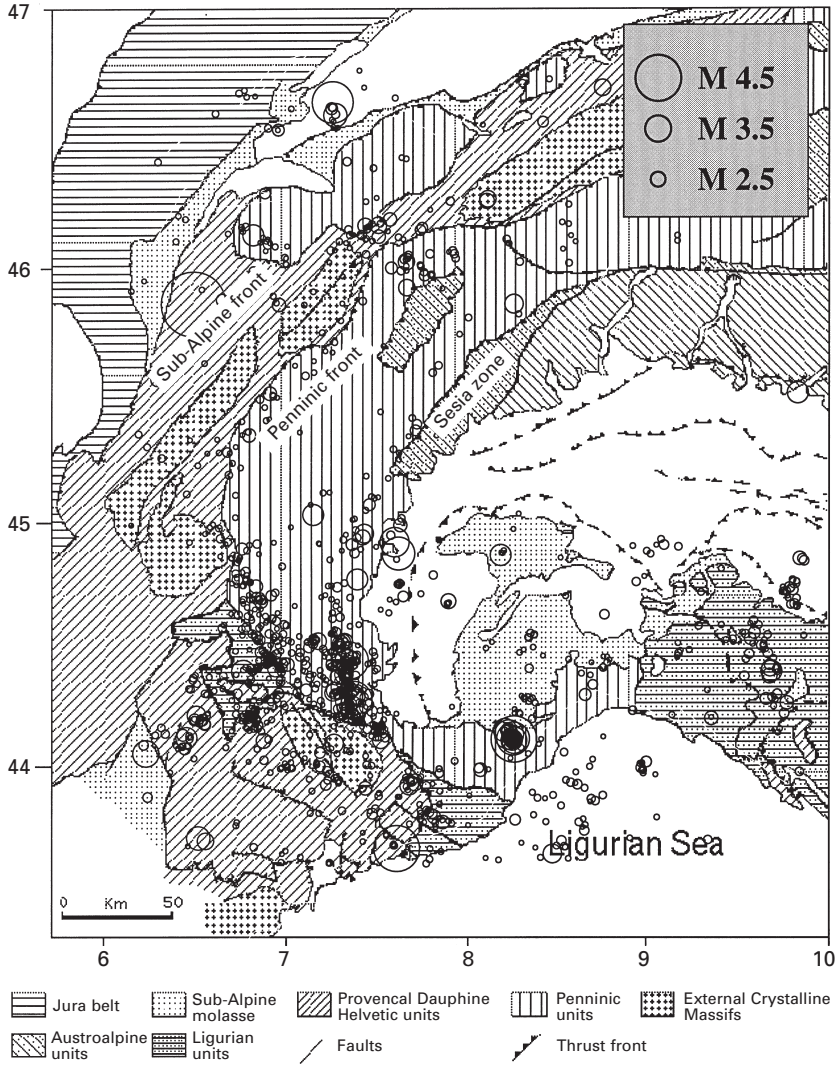

Figure 1. Seismicity from 1983 to 1996 in the western Alpine arc. Events have magnitude >2.5; Erh, Erz <5 km. The distribution of earthquakes reflects well the tectonic structure of the area (Eva *et al.* 1997).

consequence, the distribution of the *P* and *T* axes of the focal mechanisms are still somewhat confused. Previous studies evidenced a great variability of the *P* and *T* axes: a progressive rotation of the *P* axis roughly perpendicular to the chain was proposed by Fréchet (1978) and Ménard (1988), while the priority of transcurrent and transpressive solutions was the main feature of the western Alps according to Pavoni (1986).

The knowledge that the distribution of *P* and *T* axes can differ greatly from that of the principal stress directions leads us to realize that even if we were able to clear up any doubt about the behaviour of the *P* and *T* axes, this could not be considered as providing a conclusive account of the distribution of stresses affecting this sector of the Alps.

In recent work (Eva *et al.* 1997) we presented our first attempt at computing the stress tensor orientation by the inversion of fault plane solutions for the southwestern Alpine sector. In that study we came to the conclusion that, as the scale of geodynamic processes under investigation is controlled by the range of magnitudes of the events used (Rebai, Philip & Taboada 1992), we could not compute a 'regional' stress behaviour but only a local regime. We add here that, because the magnitudes of events do not exceed 5.3 (except for two events in the Ligurian Sea, estimated to be 6.0), we can only determine local regimes for the different subareas and subsets into which the western sector of the Alps and the Ligurian Sea can be divided.

This work represents a more detailed evaluation of the various stress regimes acting in a wider area of the western Alps. Through the results we can confirm, as stated by Rebai *et al.* (1992), that variations of stress directions are present in the western Alpine arc and that we have defined exactly their orientations. Determination of the changes of the stress tensor over this area and their comparison with the available information on local tectonics are the main goals of our investigation.

DATA COLLECTION

The development in the last two decades of several seismic networks [in France, Renass (Strasbourg), Sismalp (Grenoble) and LDG (Paris); in Switzerland, ETH (Zürich); and in Italy, IGG (Genoa) and ING (Rome)] over the whole area under

study allowed us to compute high-quality focal mechanisms down to a magnitude of 2.5 for the principal events.

The fault plane solutions were compiled into a database made from directly computed focal solutions and focal solutions taken from the literature. Both groups of solutions include focal mechanisms computed using the first-motion technique. In particular, computed focal solutions were obtained by means of the FPFIT code (Reasenberg & Oppenheimer 1985), which searches for the double-couple fault plane solution that best fits a given set of observed first-motion polarities for an earthquake.

The choice of including in our database focal solutions taken from the literature is useful to complete the data set, although some problems may arise from this option. In fact, it is not directly possible to estimate a quality factor for these events, and thus a selection among the available published mechanisms is necessary as a prerequisite for their usage. This selection and weighting of solutions was performed by evaluating all available information: the polarity distribution on the focal sphere, estimates of quality parameters, and the network configuration used for hypocentre and focal-mechanism computations.

Out of the 86 solutions used, with a local magnitude ranging between 2.5 and 5.3, 44 were taken from the literature (grey-shaded) (Fréchet & Pavoni 1979; Béthoux *et al.* 1988; Deverchere *et al.* 1991; Madeddu, Béthoux & Stephan 1996; Maurer 1997; Menard 1988; Nicolas, Santoire & Delpech 1990). The uncertainties of the fault parameters for these events were evaluated and found not to exceed, in general, about 20°.

The remaining 42 focal mechanisms were taken from those computed at DISTER (Dipartimento di Scienze della Terra, University of Genoa) for events occurring in the period 1980–1997, except for a few cases of older suitable events. They were selected on the basis of the restrictive criteria of a magnitude >2.5, a minimum of 20 polarities and a reasonable azimuthal coverage of stations (gap $<70°$). The DISTER solutions selected for stress inversion show fault parameter uncertainties not greater than 15–20°.

METHOD AND ANALYSIS

To compute the stress inversion from the focal solutions, we applied the method of Gephart & Forsyth (Gephart & Forsyth 1984; Gephart 1990a,b). This methodology is well known and a complete description is beyond the scope of this work. Briefly, under the basic assumption that the deviatoric stress tensor is uniform over a given rock volume and time interval, this method inverts the parameters of the focal mechanisms of earthquakes to compute the orientations of the main stress axes σ_1, σ_2 and σ_3, which are estimated together with the value of the R parameter $[=(\sigma_2-\sigma_1)/(\sigma_3-\sigma_1)]$. The program finds the solution corresponding to a minimum average misfit (F), regarded as the discrepancy between the stress tensor and the observations (fault plane solutions). The misfit of a single focal mechanism is defined as the minimum rotation about any arbitrary axis that brings one of the nodal planes and its slip vector into an orientation that is consistent with the stress model.

The value of the minimum average misfit, together with the confidence limits of the solution, computed by a statistical procedure described by Parker & McNutt (1980) and Gephart & Forsyth (1984), gives an *a posteriori* estimation of the quality of the results and provides a guide to decide whether the area considered is in a homogeneous stress field. In fact, the

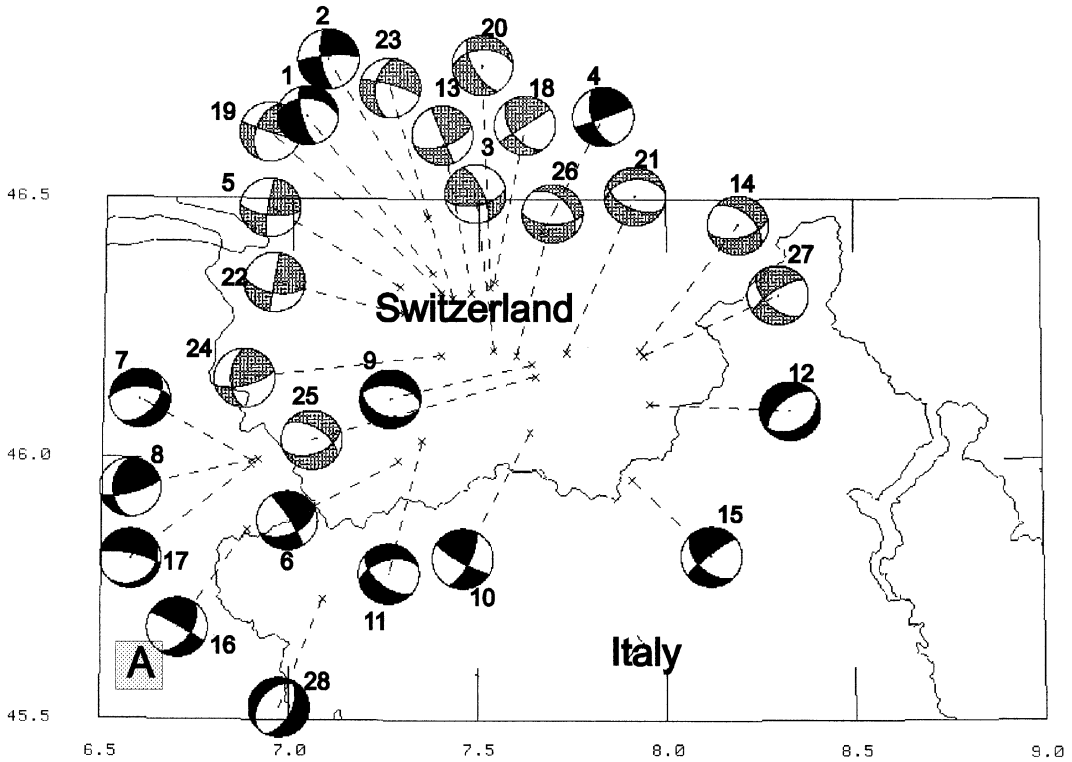

Figure 2. Focal solutions for zone A (28 events): black, computed; grey, collected from literature.

confidence limits of the solution generally tend to become larger for increasing stress heterogeneity and can also be an important *a posteriori* indicator of the suitability for stress inversion of the FPS data set.

According to Wyss *et al.* (1992) and Lu, Wyss & Pulpan (1997), *F*-values not larger than 3°, 6° and 8° are related to errors of 5°, 10° and 15°, respectively, in the focal-mechanism parameters. The errors in the focal-mechanism parameters in our FPS data set are estimated to be of the order of 15–20°, so *F*-values not exceeding 8° are assumed as a condition of a homogeneous stress tensor in the present study.

As the scale of the geodynamic processes under investigation is controlled by the magnitude range of the events used, it is very important to consider areas where the stress field is homogeneous. Defining subsectors where the stress is hypothesized to be homogeneous is a sort of 'trial and error' technique based on several *a priori* and *a posteriori* criteria. Although there is no real rule, some important parameters can influence the initial choice, but can be disclaimed or confirmed after an inversion run. Among the *a priori* parameters there are the structural pattern and the seismicity and focal-solution distributions; the *a posteriori* parameters are linked to the results of computation and depend on the value of *F* (averaged minimum misfit) and of the confidence limits.

In a first attempt, we divided the studied area into three subsectors (Zone A: south Valais and northwestern Italy; Zone B: southwestern Alps; Zone C: western Ligurian Sea) (Figs 2–4). In the following, we describe results obtained from the inversion of fault plane solutions for the various subdivisions.

RESULTS OF INVERSION

Zone A

For zone A (Fig. 2) we used 28 focal solutions, of which 14 were taken from the literature (Nicolas *et al.* 1990; Maurer 1997) and 14 were computed at DISTER (Table 1). The quality of the focal solutions is fair and we estimate the uncertainty of the positions of the nodal planes as 15°–20°. The stress inversion gave meaningful results for the analysed area. The *F*-value (5.92°), taking into account the results of Wyss *et al.* (1992) and Lu *et al.* (1997), indicates that the stress can be considered uniform and the 90 per cent and 50 per cent confidence limits of the solutions indicate very constrained solutions. Fig. 5 evidences an almost vertical σ_1 and a nearly horizontal NNW–SSE σ_3. The *R*-value (0.3) indicates that in both volumes the amplitude of σ_2 lies in the middle of the range defined by the amplitudes of σ_1 and σ_3.

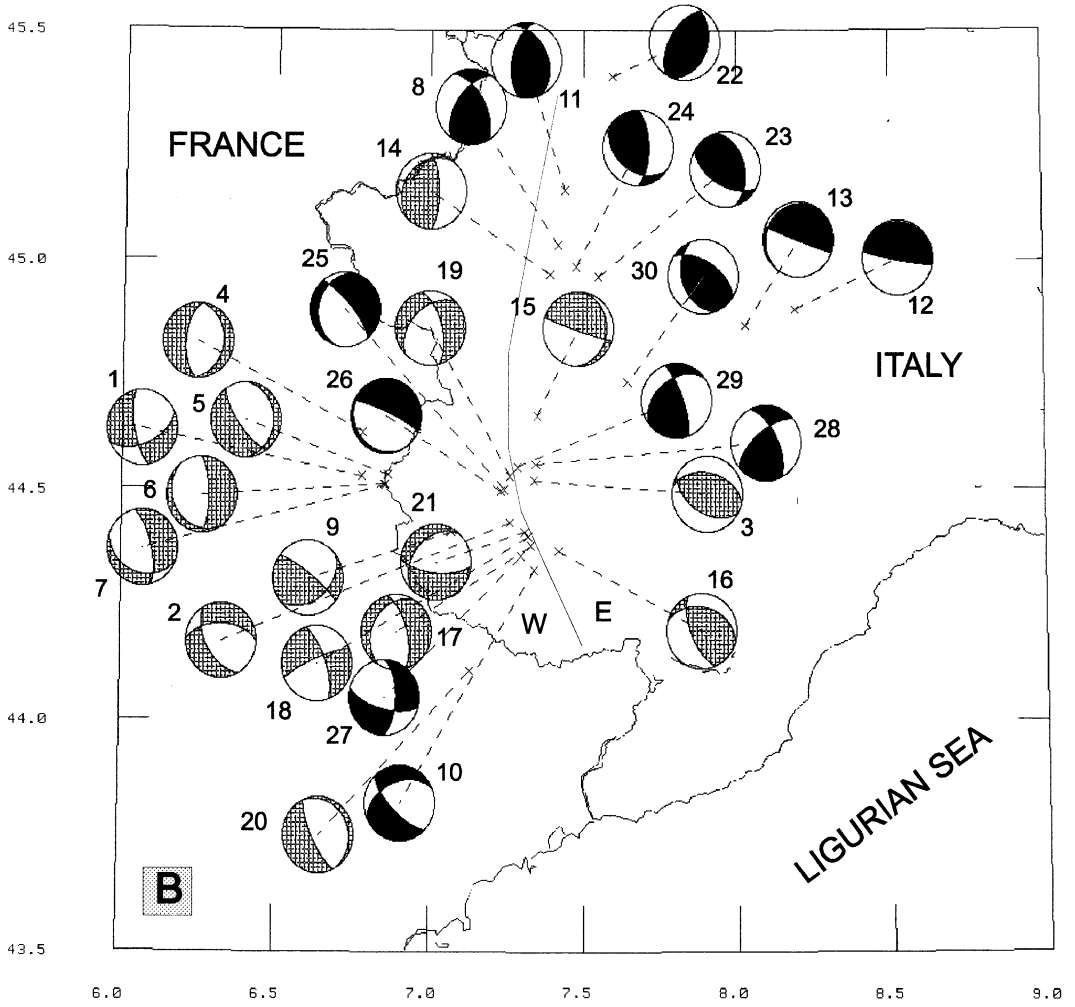

Figure 3. Focal solutions for zone B (30 events). After a first attempt, this sector was subdivided into two subzones, east (E) and west (W) [see text or Eva *et al.* (1997) for details].

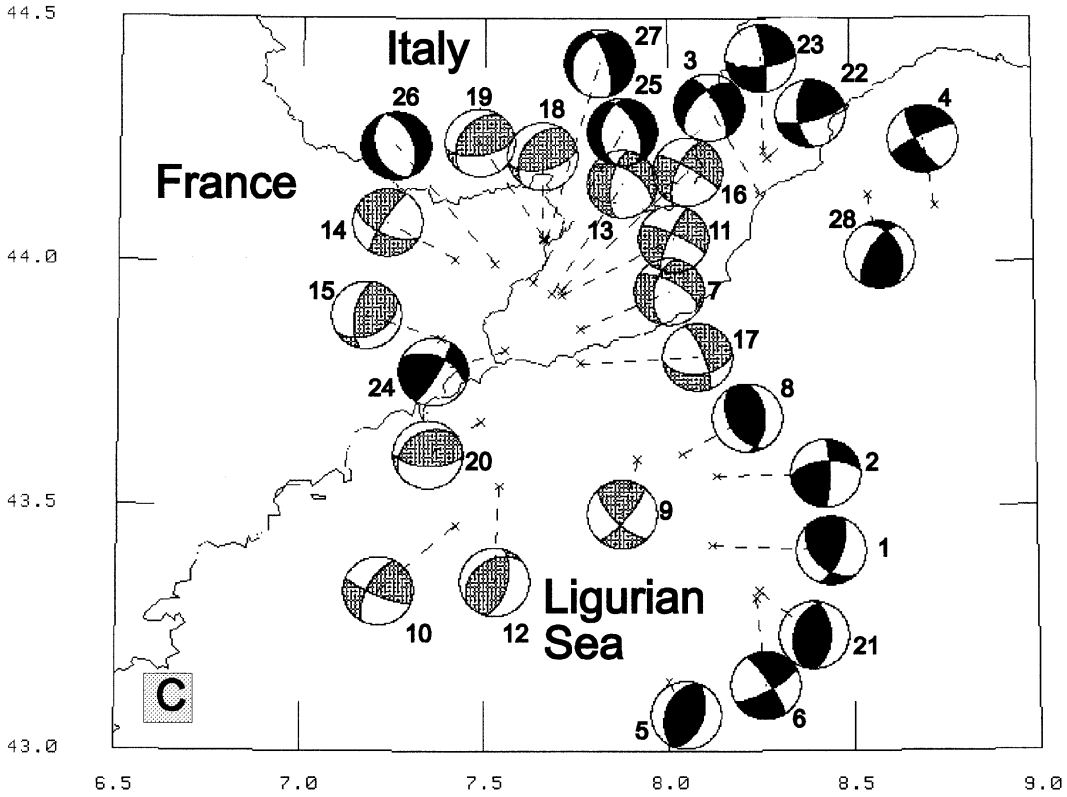

Figure 4. Focal solutions for zone C (28 events).

Zone B

For zone B (Fig. 3), in the first attempt, the entire set of fault plane solutions, composed of 16 focal mechanisms taken from the literature and 14 computed at DISTER (Table 2), was inverted for stress. The fairly large value of misfit ($F = 13.4°$) showed that no uniform stress distribution could explain the whole set of data. The data set was therefore subdivided into two parts, one consisting of the earthquakes of the external (west) side of the southwestern Alpine chain, and the other consisting of the earthquakes of the inner (east) side (Eva *et al.* 1997). In these two sectors, the focal mechanisms indicate different deformation styles. Reverse mechanisms prevail in the eastern part (labelled E in Fig. 3), in contrast to normal faulting to the west (labelled W in the same figure). The stress inversion gave meaningful results for both the western and the eastern zone. Fig. 5 shows the orientations of the maximum and minimum compressive stress (σ_1 and σ_3) for the two areas and also displays the 90 per cent confidence limits of the solutions. The F-values (7.5° and 5.4° for the western and eastern zones, respectively) indicate that the stress can be assumed to be uniform in the corresponding volumes. Fig. 5 shows a high-dip σ_3 and a nearly horizontal E–W σ_1 in the east, and reveals that σ_1 is almost vertical in the west, where σ_3 is E–W orientated with a dip of approximately 0°–20°.

Zone C

The last sector (Fig. 4) is the area of the western Ligurian region and the western Ligurian Sea. For this area we took into account 28 focal mechanisms, of which half were taken from the literature (Table 3). The inversion results give an F-value of 7.1°, which represents a homogeneous stress in the area, and the 90 per cent and 50 per cent confidence limits (Fig. 5) show solutions that are not scattered, with the principal axes of σ_1 and σ_3 orientated NW–SE almost horizontally, and NE–SW with a dip of around 30°–40°, respectively.

DISCUSSION

The stress inversion results, reported in summary in Fig. 6, appear to be in agreement with the geodynamic information available for the study area. The structural pattern of the northwestern Alps is supposed to be the product of the interaction between Adria and Europe (see for example Steck & Hunziker 1994). The anti-clockwise rotation of the Adriatic indenter relative to Europe produces a force system trending E–W in the Po plain and N–S in the northern part of the western Alps. This force system causes crustal shortening, thrusting, an accretionary wedge of soft crust in the front of the northwestern Alpine belt and strong uplift along the crest of the chain (Bernoulli, Heitzmann & Zingg 1990; Doglioni 1992, 1993). In the areas A and B the uplift is high.

The earthquakes used for stress inversion were located in the depth range 0–10 km for zone A. The fairly low misfit value obtained ($F = 5.92°$) indicates stress homogeneity. The 90 per cent confidence limit of the solution is fairly small and shows, in particular, a satisfactory level of constraint on the orientations of the principal axes of stress: a high-dip σ_1 is found. The R-values (0.3) indicate that the σ_2 amplitude is nearly equidistant from the σ_1 and σ_3 values.

The stress inversion results, together with the hypocentre distribution, give further support to local geodynamic models that assume a regional compression in the area under study,

Table 1. Locations and focal-mechanism parameters for the 28 events in zone A.

No.	Date and time	Lat.	Long.	Depth	Mag.	Plane A		Plane B		P Axis		T Axis		W	Source of data
						Az	Dip	Az	Dip	Az	Dip	Az	Dip		
1	651024 1215 56.50	46N21.36	7E22.62	10.00	4.40	165	75	92	42	115	45	226	20	1	DISTER
2	67 324 1737	46N27.72	7E21.78	10.00	4.30	265	80	171	70	130	21	37	7	1	DISTER
3	680708 0545 34.90	46N12.60	7E32.40	5.00	4.00	79	58	156	70	30	8	294	38	1	Nicolas, Santoire & Delpech 1990
4	70 818 425 31.7	46N26.22	7E40.14	10.00	4.20	160	60	69	88	119	19	20	22	1	DISTER
5	810926 1354 46.10	46N19.80	7E17.40	5.00	4.40	189	83	96	67	321	11	55	21	1	Nicolas, Santoire & Delpech 1990
6	850104 1657 37.41	45N59.71	7E17.24	10.00	3.20	65	50	149	82	279	33	23	21	2	DISTER
7	850525 1039 57.08	45N59.94	6E54.78	4.00	3.00	75	75	182	42	136	20	25	45	2	DISTER
8	860117 7 5 30.60	45N59.27	6E53.71	3.00	3.40	50	20	102	77	211	55	359	31	2	DISTER
9	860119 654 36.17	46N10.98	7E38.40	6.00	3.00	110	40	97	51	143	82	13	5	2	DISTER
10	860215 143 6.55	46N 3.06	7E38.26	6.00	3.60	120	80	26	70	252	7	345	21	2	DISTER
11	860226 13 7 16.85	46N 2.01	7E20.99	8.00	2.90	130	55	254	51	99	58	193	2	2	DISTER
12	860609 1758 38.94	46N 6.38	7E57.47	10.00	2.60	60	35	228	56	113	78	323	10	2	DISTER
13	861009 1009 54.00	46N19.20	7E28.80	5.00	3.40	69	61	159	91	290	21	28	19	2	Maurer *et al.* 1997
14	870322 136 46.00	46N12.60	7E55.80	10.00	2.60	131	51	76	55	286	59	193	2	2	Maurer *et al.* 1997
15	870530 1945 18.90	45N57.68	7E54.52	9.00	2.70	135	50	231	82	101	33	357	21	2	DISTER
16	880611 2244 45.82	45N51.67	6E53.16	8.00	3.40	120	85	34	50	249	31	354	23	2	DISTER
17	880804 1035 58.77	45N59.69	6E53.87	3.00	2.40	40	45	270	57	234	62	337	7	2	DISTER
18	890107 229 41.00	46N20.40	7E32.40	8.00	3.80	145	50	236	89	108	28	3	26	2	Maurer *et al.* 1997
19	890930 441 2.00	46N19.20	7E24.00	8.00	3.80	200	50	109	89	162	26	57	28	2	Maurer *et al.* 1997
20	900428 2224 56.00	46N19.80	7E31.80	4.00	2.50	266	46	150	66	107	52	212	12	2	Maurer *et al.* 1997
21	900511 816 22.00	46N12.30	7E44.00	6.00	2.80	263	40	115	55	77	72	191	8	2	Maurer *et al.* 1997
22	900603 1927 26.00	46N16.80	7E18.00	2.00	2.40	100	60	189	91	321	21	59	20	2	Maurer *et al.* 1997
23	900726 1230 14.00	46N18.60	7E25.80	6.00	2.40	187	50	105	80	154	35	50	19	2	Maurer *et al.* 1997
24	900831 1057 6.00	46N12.00	7E24.00	9.00	2.50	181	53	75	70	132	11	32	42	2	Maurer *et al.* 1997
25	900925 519 1.00	46N09.60	7E39.00	8.00	2.80	70	50	124	55	273	60	8	3	2	Maurer *et al.* 1997
26	901217 2334 45.00	46N12.00	7E36.00	8.00	2.40	139	41	91	60	312	63	201	10	2	Maurer *et al.* 1997
27	910907 1809 21.00	46N12.00	7E56.40	11.00	2.70	135	55	237	74	101	37	2	12	2	Maurer *et al.* 1997
28	950421 1819 31.14	45N43.89	7E 5.20	3.00	2.90	25	55	222	36	261	77	122	9	1	DISTER

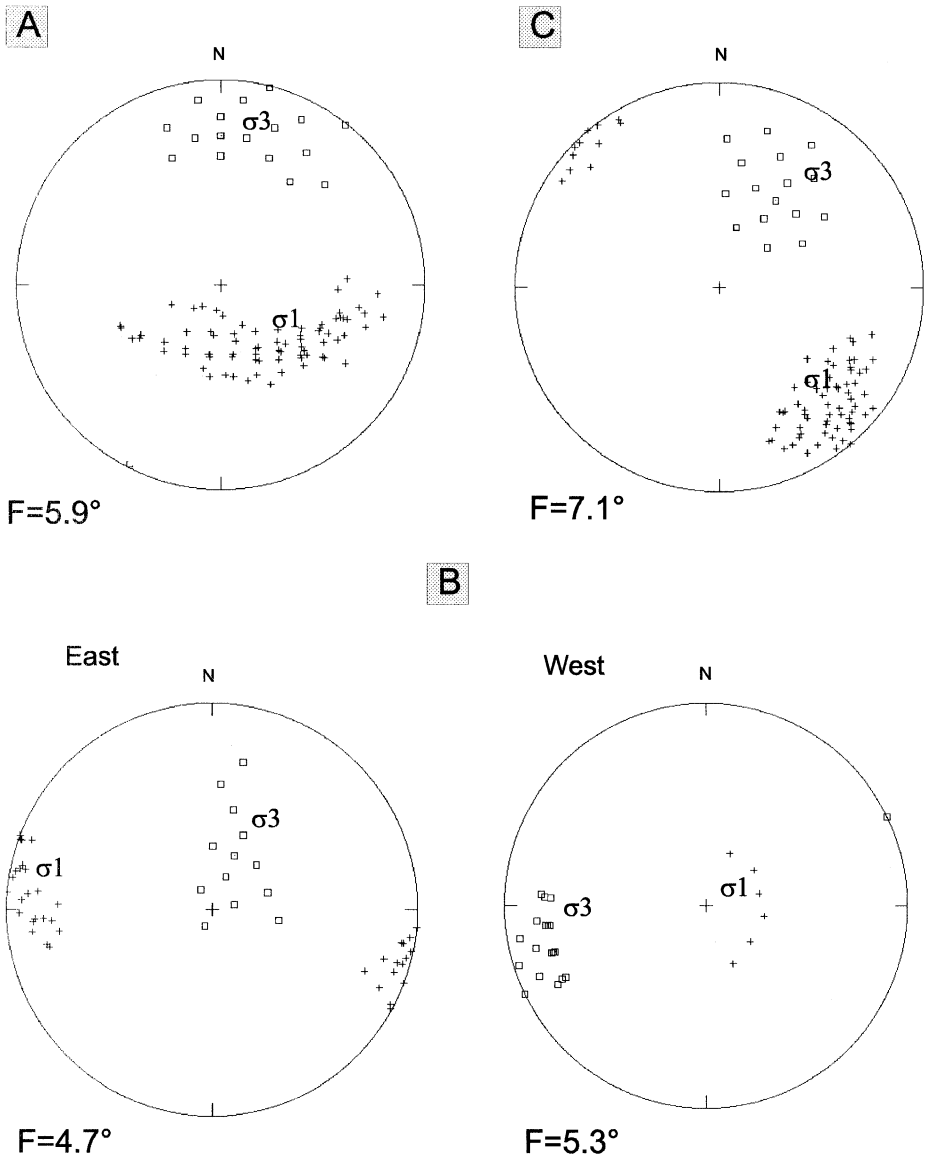

Figure 5. Summary of 90 per cent confidence limits computed for results of inversion runs.

deriving from the Adria–Europe interaction, and producing secondary tensional effects at very shallow depths. According to Molnar & Lyon-Caen (1988), one of the forces that opposes the push of two plates is gravity. Potential energy is thus stored in each column of rock, while the elevation of the chain increases to a mean value related to the force at which the plates are pushed together. When the maximum elevation is reached, convergence continues but the crest of the chain can locally undergo crustal extension.

These effects are confirmed also by the results obtained for zone B, where the *R*-values (0.5 and 0.6 for the western and eastern parts, respectively) (Table 4) indicate that in both volumes the σ_2 amplitude lies in the middle of the range defined by the σ_1 and σ_3 amplitudes. Thus, in the west the stress in the E–W direction (minimum compressive stress) is significantly smaller than in the N–S direction (an intermediate stress), in agreement with the preferentially N–S trend of the normal fault systems present in this specific volume (Labaume, Ritz & Philip 1989). Similarly, in the east, the stress in the vertical direction (minimum) is smaller than in the N–S direction (intermediate), in agreement with the E–W thrusting assumed for the same volume by local geodynamic models (Bernoulli *et al.* 1990; Doglioni 1992, 1993).

The stress inversion results reported in Fig. 6 and Table 4 appear to be in agreement with the geodynamic uplift associated with the regional-scale thrusting process, which has reactivated, as normal faults, pre-existing shallow structures (Labaume *et al.* 1989). For the Ligurian Sea subzone, the results of inversion show a rotation of the principal stress axes with respect to the western Alps and correspond to an area with a NW–SE compressive trend. This compressive regime can be associated with the closing direction of the Ligurian Sea (Réhault & Béthoux 1984).

CONCLUSIONS

Stress inversion from 86 earthquake fault plane solutions of the western Alps (depth <25 km) shows different orientations

Table 2. Locations and focal-mechanism parameters for the 30 events in zone B.

No.	Date and time	Lat.	Long.	Depth	Mag.	Plane A		Plane B		P Axis		T Axis		W	Source of data
						Az	Dip	Az	Dip	Az	Dip	Az	Dip		
1	590405 1048 0.00	44N31.80	6E46.80	0.00	5.3	170	72	66	54	34	39	295	11	2	Ménard 1988
2	710201 1226 6.20	44N25.80	7E15.60	2.00	4.3	150	55	92	53	120	56	211	1	2	Nicolas *et al.*1990
3	770206 1601 2.70	44N31.20	7E20.40	10.00	4.0	120	48	102	43	202	2	97	81	2	Ménard 1988
4	770916 1827 0.00	44N37.45	6E47.09	3.10	2.5	6	29	186	61	96	74	276	16	1	Fréchet & Pavoni 1979
5	770923 0241 0.00	44N31.96	6E51.96	2.00	2.5	0	22	145	72	36	61	245	26	1	Fréchet & Pavoni 1979
6	780930 0913 0.00	44N30.75	6E51.24	5.90	2.5	0	74	145	19	285	60	81	28	1	Fréchet & Pavoni 1979
7	780930 0941 0.00	44N30.65	6E51.46	7.70	2.5	167	70	111	33	293	57	57	20	1	Fréchet & Pavoni 1979
8	800105 1431 29.90	45N 2.04	7E25.14	4.00	4.8	215	55	151	58	92	2	185	51	1	DISTER
9	801010 2142 52.10	44N24.60	7E04.20	5.00	4.2	128	80	51	39	9	25	254	42	2	Nicolas, Santoire & Delpech 1990
10	810104 0409 0.00	44N19.68	7E20.46	5.00	3.5	135	70	247	44	88	49	197	15	1	DISTER
11	810208 0430 10.50	45N 9.12	7E26.34	5.00	4.4	155	40	192	56	266	9	153	69	1	DISTER
12	820805 1654 0.00	44N53.52	8E11.46	5.00	3.7	100	85	100	5	190	40	10	50	2	DISTER
13	820806 1328 35.20	44N51.42	8E 1.68	10.00	4.4	30	45	260	57	224	62	327	7	2	DISTER
14	830906 2243 18.40	44N58.20	7E23.40	5.00	3.8	0	72	221	23	102	26	248	60	2	Nicolas, Santoire & Delpech 1990
15	840112 0824 46.40	44N39.60	7E21.00	10.00	3.6	5	20	108	85	215	37	358	46	1	Béthoux *et al.* 1988
16	850221 1800 34.50	44N22.20	7E25.20	14.00	3.2	157	65	105	37	227	15	108	60	1	Béthoux *et al.* 1988
17	860117 1848 03.90	44N22.80	7E19.80	10.00	3.3	210	33	165	65	219	63	92	17	2	Béthoux *et al.* 1988
18	860311 0746 37.80	44N24.00	7E19.20	5.00	3.6	247	79	161	69	203	23	295	7	2	Béthoux *et al.* 1988
19	860717 0735 34.10	44N31.80	7E15.60	1.00	3.2	225	45	166	63	207	55	102	10	2	Béthoux *et al.* 1988
20	860818 1137 11.90	44N06.60	7E07.80	6.00	3.2	155	75	155	15	65	60	245	30	2	Béthoux *et al.* 1988
21	870615 2127 18.10	44N24.60	7E18.60	10.00	3.3	222	35	96	67	44	58	166	18	2	Béthoux *et al.* 1988
22	870703 1046 57.03	45N23.94	7E35.73	3.00	3.7	20	35	212	56	297	10	147	78	2	DISTER
23	900211 0700 37.78	44N57.90	7E32.84	16.00	4.2	120	55	165	45	231	6	333	65	1	DISTER
24	900211 0707 47.81	44N59.23	7E28.54	24.00	2.7	0	65	126	38	69	15	313	59	1	DISTER
25	921027 0312 31.60	44N30.11	7E14.57	8.71	2.9	140	75	195	25	205	56	66	27	1	DISTER
26	921111 059 53.35	44N29.87	7E13.96	8.56	2.6	145	10	115	81	199	53	29	36	1	DISTER
27	930315 2343 29.63	44N21.55	7E17.86	13.94	4.3	105	65	1	63	324	38	233	1	1	DISTER
28	940120 0659 14.36	44N33.67	7E20.28	4.84	4.7	220	75	147	42	281	20	170	45	1	DISTER
29	940120 0705 42.99	44N32.84	7E16.82	14.09	4.3	160	75	237	51	104	15	207	39	1	DISTER
30	950304 0158 13.81	44N44.05	7E38.67	25.12	4.3	160	40	123	56	56	9	162	69	1	DISTER

Table 3. Locations and focal-mechanism parameters for the 28 events in zone C.

No.	Date and time	Lat.	Long.	Depth	Mag.	Plane A		Plane B		P Axis		T Axis		W	Source of data
						Az	Dip	Az	Dip	Az	Dip	Az	Dip		
1	630719 0544 00.00	43N25.20	8E 7.20	8.00	6.00	20	65	137	46	82	11	338	52	1	DISTER
2	630727 0557 00.00	43N33.60	8E 7.80	14.00	6.00	0	80	264	61	129	13	226	28	1	DISTER
3	701230 0220 00.00	44N08.28	8E15.18	5.00	4.00	224	52	330	70	193	42	93	11	1	DISTER
4	710925 1034 00.00	44N 7.02	8E43.80	5.00	4.20	150	75	243	80	107	18	16	4	1	DISTER
5	810105 0810 00.00	43N 8.46	8E00.00	10.00	3.60	20	50	200	40	110	5	290	85	1	DISTER
6	810422 0426 20.60	43N18.78	8E14.16	2.00	4.60	60	75	147	80	283	18	14	4	1	DISTER
7	831204 1734 51.90	43N51.60	7E45.60	1.00	3.50	190	54	120	65	160	46	63	6	1	Bethoux *et al.* 1988
8	851004 1317 21.53	43N36.24	8E 2.30	15.00	4.10	150	45	177	48	74	2	337	76	1	DISTER
9	851005 1558 40.60	43N37.20	8E02.40	16.00	3.10	40	77	135	70	88	5	356	24	1	Béthoux *et al.* 1988
10	860501 0028 02.10	43N27.60	7E25.20	10.00	3.90	208	64	112	78	162	10	67	27	1	Béthoux *et al.* 1988
11	861020 2029 11.30	43N55.80	7E42.60	2.00	3.00	203	79	115	79	159	16	69	0	1	Béthoux *et al.* 1988
12	891226 1959 59.10	43N32.40	7E32.40	10.00	4.50	15	60	231	36	119	13	244	68	1	Béthoux *et al.* 1988
13	900702 1842 00.00	43N56.00	7E41.00	2.00	2.70	190	63	122	53	152	48	248	6	1	Deverchere *et al.* 1991
14	900809 1916 57.61	44N00.00	7E25.20	6.00	3.2	116	60	212	80	78	29	341	13	1	Madeddu, Béthoux & Stephan 1997
15	900908 0831 22.91	43N50.40	7E22.80	11.00	2.7	60	40	190	62	301	12	53	61	1	Madeddu, Béthoux & Stephan 1997
16	901002 0206 24.12	43N56.40	7E42.60	11.00	2.9	300	80	205	64	165	26	70	11	1	Madeddu, Béthoux & Stephan 1997
17	910205 0906 10.39	43N47.40	7E45.60	8.00	3.0	339	75	83	48	296	40	37	17	1	Madeddu, Béthoux & Stephan 1997
18	910219 1533 00.00	44N02.60	7E39.50	7.00	2.9	215	40	77	58	149	10	36	66	1	Madeddu, Béthoux & Stephan 1997
19	910225 1130 11.80	44N02.90	7E39.60	4.00	3.3	215	40	80	59	151	10	38	64	1	Madeddu, Béthoux & Stephan 1997
20	910628 2348 48.00	43N40.20	7E29.40	5.00	2.9	92	62	237	33	169	15	38	68	1	Madeddu, Béthoux & Stephan 1997
21	920921 1237 04.03	43N19.67	8E14.67	19.70	3.00	0	50	195	41	97	5	217	81	2	DISTER
22	930717 1035 00.60	44N13.29	8E15.15	7.80	4.50	165	65	71	81	120	11	25	24	2	DISTER
23	930717 1108 23.17	44N13.64	8E15.74	8.90	3.70	85	70	172	81	307	21	40	7	1	DISTER
24	950421 0802 57.48	43N48.93	7E33.38	4.00	4.30	30	80	112	51	155	19	259	35	2	DISTER
25	960926 2137 36.70	43N57.37	7E37.84	7.20	2.70	187	40	335	55	194	72	79	8	1	DISTER
26	961017 1521 38.80	43N59.72	7E31.72	10.50	3.20	160	40	34	50	250	85	70	5	1	DISTER
27	961124 0027 08.10	44N02.67	7E40.07	2.60	3.50	184	20	344	71	226	59	89	23	1	DISTER
28	961125 1947 23.20	44N08.34	8E32.79	3.00	3.80	335	40	212	66	278	14	165	58	1	DISTER

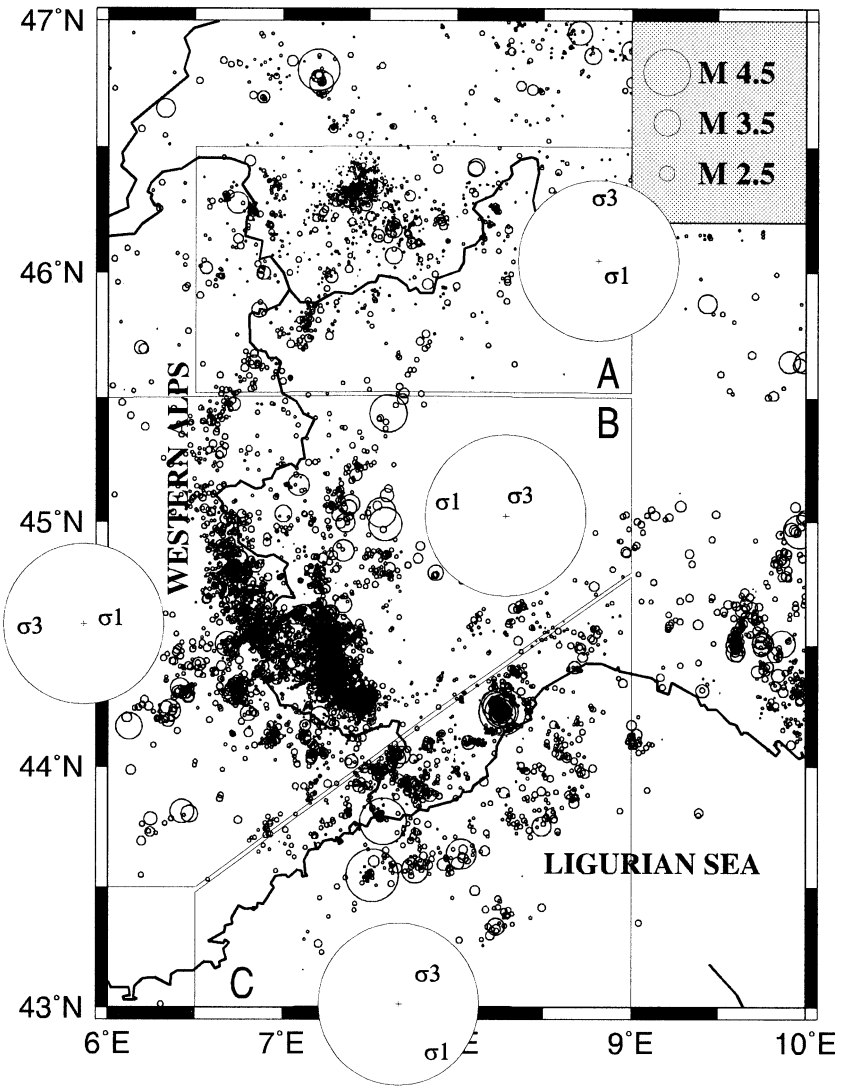

Figure 6. Distribution of stress orientations in western Alpine arc for subzones A, B and C as derived from the present work. All earthquakes 1983–1996 are shown.

Table 4. Summary of results of inversion runs. For the meaning of B/East and B/West, see text. N is the number of focal solutions used for inversion, F is the misfit and $R=(\sigma_2-\sigma_1)/(\sigma_3-\sigma_1)$.

Set	N	F	σ_1		σ_2		σ_3		R
			Dip	Strike	Dip	Strike	Dip	Strike	
A	28	5.9°	59	153	12	263	28	0	0.3
B/West	16	5.3°	66	54	7	160	23	253	0.5
B/East	14	4.7°	5	282	22	180	67	23	0.6
C	28	7.1°	16	142	37	245	48	33	0.5

of the principal stress axes (σ_1 and σ_3) for the various subzones into which we divided the area. These orientations are characterized by slight to significant deviations from the expected compressional force due to the collision between the Adriatic and European plates. Several local stress fields are superimposed on, or partly derived from, this more regional compressive force.

In both the northern and the southern sectors of the western Alpine arc (zones A and B), the gravitational collapse occurring during the orogenesis (Molnar & Lyon-Caen 1988) is responsible for a local distensive stress regime accompanied by shallow earthquakes. In the northern part (zone A), the stress orientation is rotated by almost 90° with respect to the southern sector as a consequence of the bending of the Alpine chain.

For the southern zone (zone B), the availability of a greater number of events allowed us to perform two inversions, one using shallow events, whose result is a distensive local stress

regime, and one performed with deeper events, showing a compressive E–W-orientated stress field.

In the case of the Ligurian Sea, the stress regime can be considered as the consequence of the collision between the African and European plates along a N–S direction, and has the same properties of that of western Europe (Mueller *et al.* 1992). In this sense, the general behaviour of the Ligurian Sea should be considered independently from the Alpine chain. Compression in the Ligurian Sea could also be responsible for the triggering of the reactivation of the complex system of faults in the Nice arc and for the seismicity of the northern margin of the Ligurian Sea.

ACKNOWLEDGMENTS

We are indebted to Hervé Philip and two anonymous reviewers, who improved the manuscript with their valuable suggestions.

REFERENCES

Bernoulli, D., Heitzmann, P. & Zingg, A., 1990. Central and southern Alps in southern Switzerland. Tectonic evolution and first results of reflection seismics, in *Deep Structure of the Alps,* pp. 289–302, ed. Roure F., Heitzmann P. & Polino R., *Mém. Soc. géol. Fr., Paris,* **156**; *Mém. Soc. géol. Suisse, Zürich,* **1**; *Vol. spec. Soc. Geol. It., Roma,* **1**.

Béthoux, N., Cattaneo, M., Delpech, P.Y., Eva, C. & Rehault, J.P., 1988. Mécanismes au foyers des séismes en mer ligure et dans le Sud des Alpes occidentales: résultats et interprétation, *C. R. Acad. Sci. Paris,* **307,** 71–78.

Deverchere, J., Béthoux, N., Hello, Y., Loaut, R. & Eva, C., 1991. Déploiement d'un réseau de sismographes sous-marins et terrestres en domaine Ligure (Méditerranée): campagne SISBALIG I, *C. R. Acad. Sci. Paris,* 313, Serie II, 1023–1030.

Doglioni, C., 1992. Main differences between thrust belts, *Terra Nova,* **4,** 152–164.

Doglioni, C., 1993. Some remarks on the origin of foredeeps. *Tectonophysics,* **228,** 1–20.

Eva, C., Augliera, P., Cattaneo, M. & Giglia, G., 1990. Some considerations on seismotectonics of northwestern Italy, in *The European Geotraverse: Integrative Studies,* pp. 289–296, eds R. Freeman, P. Giese and S. Mueller, European Science Foundation, Strasbourg.

Eva, E., Solarino, S., Eva, C. & Neri, G., 1997. Stress tensor orientation derived from fault plane solutions in the southwestern Alps, *J. geophys. Res.,* **102,** 8171–8185.

Fréchet, J., 1978. Sismicité du sud-est de la France, et une nouvelle méthode de zonage sismique, *PhD Thesis,* University of Science, Technology and Medicine, Grenoble.

Fréchet, J. & Pavoni, N., 1979. Etude de la sismicité de la Zone briançonnaise entre Pelvoux et Argentera (Alpes Occidentales) à l'aide d'un réseau de stations portables, *Eclogae geol. Helv.,* **72/3,** 763–779.

Gephart, J.W., 1990a. Stress and the direction of the slip on fault plane, *Tectonics,* **9,** 845–858.

Gephart, J.W., 1990b. FMSI: a Fortran program for inverting fault/slickenside and earthquake focal mechanism data to obtain the regional stress tensor, *Comp. Geosci.,* **16,** 953–989.

Gephart, J.W. & Forsyth, W.D., 1984. An improved method for determining the regional stress tensor using earthquake focal mechanism data: applications to the San Fernando earthquake sequence, *J. geophys. Res.,* **89,** 9305–9320.

Labaume, P., Ritz, J.F. & Philip, H., 1989. Failles normales recentes dans les Alpes sud-occidentales: leurs relations avec la tectonique compressive, *C. R. Acad. Sci. Paris,* **308,** Serie II, 1553–1560.

Lu, Z., Wyss, M. & Pulpan, H., 1997. Details of stress directions in the Alaska Subduction Zone from fault plane solutions, *J. geophys. Res.,* **102,** 5385–5402.

Madeddu, B., Béthoux, N. & Stéphan, J.F., 1996. Champ de contrainte post-pliocene et déformations récentes dans les Alpes sud-occidentales, *Bull. Soc. géol. France,* **167,** 797–810.

Maurer, H., Burkhard, M., Deichmann, N. & Green, A.G., 1997. Active tectonism in the Western Swiss Alps, *Terra Nova,* **9,** 91–94.

Mayer-Rosa, D. & Mueller, S., 1979. Studies of seismicity and selected focal mechanisms in Switzerland, *Schweiz. min. petrogr. Mit.,* **59,** 127–132.

Menard, G., 1988. Structure et cinématique d'une chaine de collision—Les Alpes occidentales et centrales, *Thesis,* Université J. Fourier, Grenoble.

Molnar, P. & Lyon-Caen, H., 1988. Some simple physical aspects of the support, structure, and evolution of mountain belts, *Geol. Soc. Am. Spec. Pap.,* **218,** 179–207.

Mueller, B., Zoback, M.L., Fuchs, K., Mastin, L., Gregersen, S., Pavoni, N., Stephansson, O. & Ljunggren, C., 1992. Regional patterns of tectonic stress in Europe, *J. geophys. Res.,* **97,** 11 783–11 803.

Nicolas, M., Santoire, J.P. & Delpech, P.Y., 1990. Intraplate seismicity: new seismotectonic data in Western Europe, *Tectonophysics,* **179,** 27–53.

Parker, R.L. & McNutt, M.K., 1980. Statistics for the one norm misfit measure, *J. geophys. Res.,* **85,** 4429–4430.

Pavoni, N., 1986. Regularities in the pattern of major fault zones of the earth and the origin of arcs, in *The origin of arcs,* pp. 63–68, ed. Wezel, F.C., Elsevier, Amsterdam.

Reasenberg, P. & Oppenheimer, D.H., 1985. FPFIT, Fortran computer program for calculating and displaying earthquake fault-plane solutions, *USGS Open File Rept,* **85–739.**

Rebai, S., Philip, H. & Taboada, A., 1992. Modern tectonic stress field in the Mediterranean region: evidence for variation in stress directions at different scales, *Geophys. J. Int.,* **110,** 106–140.

Rehault, J.P. & Béthoux, N., 1984. Earthquake relocation in the Ligurian sea (Western Mediterranean): geological interpretation, *Mar. Geol.,* **55,** 429–445.

Steck, A. & Hunziker, J., 1994. The Tertiary structural and thermal evolution of the Central Alps—compressional and extensional structures in an orogenic belt, *Tectonophysics,* **238,** 229–254.

Wyss, M., Liang, B., Tanigawa, W.R. & Wu, X., 1992. Comparison of orientations of stress and strain tensors based on fault plane solutions in Kaoiki, Hawaii, *J. geophys. Res.,* **97,** 4769–4790.